

Magnetic field induced lattice ground states from holography

Yan-Yan Bu,^{a,b} Johanna Erdmenger,^a Jonathan P. Shock,^a Migael Strydom^a

^a*Max-Planck-Institut für Physik (Werner-Heisenberg-Institut),
Föhringer Ring 6, 80805 München, Germany.*

^b*State Key Laboratory of Theoretical Physics, Institute of Theoretical Physics, Chinese Academy of Science,
Beijing 100190, People's Republic of China*

E-mail: [\(yybu,jke,jonshock,mstrydom\)mppmu.mpg.de](mailto:(yybu,jke,jonshock,mstrydom)mppmu.mpg.de)

ABSTRACT: We study the holographic field theory dual of a probe $SU(2)$ Yang-Mills field in a background $(4 + 1)$ -dimensional asymptotically Anti-de Sitter space. We find a new ground state when a magnetic component of the gauge field is larger than a critical value. The ground state forms a triangular Abrikosov lattice in the spatial directions perpendicular to the magnetic field. The lattice is composed of superconducting vortices induced by the condensation of a charged vector operator. We perform this calculation both at finite temperature and at zero temperature with a hard wall cutoff dual to a confining gauge theory. The study of this state may be of relevance to both holographic condensed matter models as well as to heavy ion physics. The results shown here provide support for the proposal that such a ground state may be found in the QCD vacuum when a large magnetic field is present.

KEYWORDS: Gauge-gravity correspondence, Holography and condensed matter physics(AdS/CMT)

Contents

| | | |
|----------|---|-----------|
| 1 | Introduction | 1 |
| 2 | Holographic setup | 4 |
| 2.1 | The finite temperature and hard wall backgrounds | 4 |
| 2.2 | The Yang-Mills action | 5 |
| 2.3 | Perturbative expansion of the gauge fields | 6 |
| 2.4 | Gauge field boundary conditions | 6 |
| 2.5 | The gauge theory ground state energy | 7 |
| 3 | Solving the equations | 8 |
| 3.1 | The comparison with Ginzburg-Landau theory | 8 |
| 3.2 | The gauge field perturbative expansion in more detail | 8 |
| 3.3 | Solving the equations to linear order | 9 |
| 3.4 | The Abrikosov lattice solution | 10 |
| 3.5 | Higher order contributions to the energy | 10 |
| 3.6 | Solving the equations to higher orders | 11 |
| 3.7 | Numerical solutions | 12 |
| 4 | Results | 13 |
| 4.1 | Finding the minimum energy state | 13 |
| 4.2 | An analysis of $P = 2$ solutions | 14 |
| 5 | Conclusion | 16 |
| A | Deriving the equations for $a_{x,y}^3$ | 17 |
| B | Deriving the equations for $c_{x,n}, c_{y,n}$ | 19 |
| C | Calculating the energy | 20 |

1 Introduction

The study of black hole instabilities is an important research topic that has led to very interesting results. In particular, within gauge/gravity duality, the study of Anti-de Sitter black hole solutions and their stability properties is important for understanding thermal states on the gauge theory side. Last year in [1], some of the authors of the present paper studied an $SU(2)$ Einstein-Yang-Mills model at finite temperature in asymptotically AdS space. They found that when a magnetic component of the gauge field reaches a critical value in units of the temperature, the system becomes unstable. Though the critical value of the magnetic field for onset of the instability was calculated, the new ground state of the system was not known. In the current work we calculate a ground state solution, using a perturbative analysis similar to the one performed by Abrikosov in [2] for type II superconductors. In agreement with the work of Abrikosov we find that the ground state is a triangular lattice. There have been many attempts recently to model lattices holographically with the goal of providing more realistic models for condensed matter systems [3, 4], and this

novel procedure for generating a lattice dynamically adds to these developments. Moreover, our holographic model provides support for recent QCD studies of ρ meson condensation from a strong magnetic field [5–7]. The effect described here is similar to the Nielsen-Olsen solution for gluon condensation [8] and to magnetically catalysed W boson condensation [9–11].

Although this is the first holographic calculation to explicitly uncover an Abrikosov lattice in 3+1 dimensions, it is not the first to examine spatially inhomogeneous phases of strongly coupled field theories. In [3], the authors studied the holographic construction of an Einstein-Maxwell-scalar theory at finite temperature and density. They looked at the gauge theory optical conductivity, which is the conductivity in the direction of an applied electric field. They broke the translational invariance explicitly by imposing scalar field boundary conditions in the form of a lattice modulated in one of the Minkowski spatial directions. A fully backreacted solution was found which thus induces a spatially inhomogeneous black hole solution. This leads to an extremely rich behaviour of the frequency dependent optical conductivity. At low frequencies there appears a Drude peak. A Drude peak is a broadening of the zero frequency delta peak in the conductivity. In real materials this is due to impurities and finite temperature effects. The Drude peak is not present when translational invariance is unbroken. The solution also exhibits a power law behaviour at frequencies intermediate with respect to the temperature, and a constant value in the high frequency regime. The power law behaviour is the same as that found experimentally in cuprates, while the constant value at high frequencies is expected from conformal invariance. The setup in this context was a (2+1)-dimensional model where the lattice was periodic in only one of the spatial dimensions. A more realistic lattice structure would be highly desirable.

While the lattice in the approach of [3] was implemented in the boundary conditions, there are a number of other mechanisms known that lead dynamically to ground states without translational symmetry. One approach was pioneered in [12] by studying a Yang-Mills-Chern-Simons theory in the gauge/gravity context. It was shown that the Chern-Simons term can induce an instability which leads to a ground state with both translational and rotational symmetry breaking. Such work was continued in [13–17] where the spatially homogeneous phase was found to be unstable in a variety of gravitational contexts in the presence of Chern-Simons couplings. The perturbative analysis of quasinormal modes that become tachyonic at finite momentum gives a relatively simple computational tool for finding instabilities to ground states without translational symmetry. These solutions are found to induce a helical current [18–20]. Interestingly, a Chern-Simons term is not always enough to induce such an instability. It was shown by [21] that this type of instability does not exist in the D3/D7 system.

Translational invariance can also be broken with a magnetic field or with magnetic monopoles. The former was first studied by Gauntlett et al. in [22] and [23] where the instability of the magnetically charged black hole in a top-down framework was studied in detail. In the latter work, an infinite family of solutions coming from $D = 11$ supergravity was shown to exhibit a magnetically catalysed instability. Such work is important as it proves that these instabilities can also come from real string theory constructions. The subject of magnetic monopoles in $(3 + 1)$ -dimensional AdS space was studied in [24] and [25]. These magnetic monopoles are solutions to the scalar field in a Yang-Mills-Higgs theory with gauge group $SU(2)$. In a certain limit where the monopole magnetic charge becomes large and a “monopole wall” is formed, it was shown in [24] that there is a W boson instability. In [25] a hexagonal lattice ground state of these monopole walls was found numerically. In [26] the holographic dual of a self-gravitating Julia-Zee Dyon was constructed, and it was shown to contain a vortex condensate.

There are some holographic models exhibiting a superconducting phase transition that results in a vortex lattice ground state. The first we mention involves an s -wave superconductor. In [27] a type II superconductor was modelled using a $(3 + 1)$ -dimensional gravitational setup. A type II superconductor is one for which the external applied magnetic field has two critical values. When

the magnitude of the magnetic field increases beyond the lower of the two critical values, the field starts to penetrate the superconducting condensate. Some of the condensate remains until the magnitude of the field is increased beyond the upper critical value, at which point superconductivity is completely destroyed. Just before the upper critical value is reached from below, the ground state of the system is a triangular Abrikosov lattice [2]. The authors of [27] constructed a holographic superconductor modelling the behaviour of a type II superconductor near the upper critical value of the magnetic field and found the Abrikosov lattice ground state explicitly.¹ In [29] it was shown how to construct a similar vortex lattice solution in a model describing a p -wave superconductor. There the authors used a holographic model with an $SU(2)$ gauge field similar to the one described in the current paper. Both of these examples are different from our model, however, because here we find a superconducting Abrikosov lattice ground state that is induced by an $SU(2)$ magnetic field, rather than being destroyed by it. Moreover, in contrast to these models, we do not need a finite density. Our model is a cousin of holographic p -wave superconductors where the condensation is induced by a finite isospin density, holographically realised by a non-trivial temporal component of the $SU(2)$ gauge field (see [30] and [31, 32] as well as the recent [33]). Here, in contrast, a spatial component of this gauge field has a non-trivial profile. Whereas in [31, 32], a Meissner effect is shown to occur by which a magnetic field reduces the transition temperature, here it is again the magnetic field which induces condensation at zero density.

In addition to being interesting in the broader context of holographic lattices, the model we discuss serves as supporting evidence for a phenomenon first described by Chernodub et al. in [5, 6]. There it was proposed that the $QCD \times QED$ vacuum may itself be susceptible to a superconducting transition when a magnetic field of the order of the QCD scale is present. Such extreme conditions are rare but they may be present for a few femtoseconds during highly off-centre heavy ion collisions. The discovery of this phase came about through the study of an effective field theory description (the DSGS model proposed by Djukanovic, Schindler, Gegelia and Scherer in [34]) of ρ mesons interacting with a magnetic field. A destabilisation of the vacuum was shown that would clearly lead to the condensation of charged and neutral ρ mesons. This breaks the $U(1)$ gauge symmetry and leads to a superconductor with the quark-antiquark pairs in the mesons acting as Cooper pairs. The instability was also found using an extended Nambu–Jona-Lasinio model with $SU(3)$ colour and $SU(2)$ flavour in [35]. Lattice gauge theory studies were then performed looking at QCD in strong magnetic fields and these indicate the same instability. Moreover, using the DSGS model and guided by the Ginzburg-Landau model of type II superconductors, a solution was found in which the ρ meson condensate forms an Abrikosov lattice made up of superconducting vortices [7]. This may be relevant experimentally. Evidence has mounted at both RHIC and the ALICE experiment at CERN that strong magnetic fields may contribute to the physics of the strongly coupled quark gluon plasma as charges are quickly accelerated during the interaction period [36, 37]. The importance of these effects remains a contested topic because the time scales involved are small. However, given that strong magnetic fields may be present, it is interesting to ask if traces of this ρ meson condensate could be detected.

In the current paper we find a possible ground state of the system in [1]. As mentioned above, this system was shown to be unstable under the imposition of a large $SU(2)$ magnetic field.² We show that it has very similar properties to the ground state of a type II superconductor near the upper critical magnetic field as well as to the ground state in the model of Chernodub et al. In other words, the ground state is a triangular Abrikosov lattice. We take here a very simple model

¹ The model of [27] does not display the transition at the lower critical magnetic field value because the gauge field is not dynamical. See [28] for adding dynamical gauge fields to holographic superconductors. The transition at the upper critical value is present however because there the condensate is small so the backreaction is negligible.

²It was shown in [38] that the same sort of instability occurs in the Sakai-Sugimoto model, but there the ground state has also not been found.

of a strongly coupled finite temperature quantum field theory in $(3+1)$ -dimensions with a global $SU(2)$ symmetry. The dual gravity theory is an $SU(2)$ Einstein-Yang-Mills theory in $(4+1)$ -dimensions with a magnetic component of the $SU(2)$ switched on. We work entirely within the probe approximation, which means that the Yang-Mills term is small compared to the Einstein-Hilbert term in the action. We also fix the gauge in such a way that the gauge theory condensate is transformed under a $U(1)$ subgroup of the global $SU(2)$ symmetry. There appears to be a certain universality to the triangular lattice ground state. Here we show that it forms in both the AdS Schwarzschild background (dual to a finite temperature field theory) as well as the hard wall cutoff model (dual to a confining field theory). It would be interesting to uncover exactly how universal these results are.

The two holographic models that we study have several important differences from QCD. In the finite temperature model there is no confinement or chiral symmetry breaking and so there are no goldstone bosons (pions) present which are the normal decay modes of the ρ meson in QCD. The hard wall model has its conformal symmetry broken only by an IR boundary condition which sets a confinement scale. However, the phenomenology of these two models appears to be close enough to that of QCD to compare qualitatively with the models of Chernodub et al.

In section 2 we provide the details of the holographic setup. There we also explain the strategy behind the perturbative expansion of the $SU(2)$ gauge field near the critical magnetic field. Since we follow the philosophy of Abrikosov's calculation of the ground state in type II superconductors, which was done in the Ginzburg-Landau model, in section 3 we give a brief outline of this approach and then follow it to solve perturbatively up to third order. In section 4 we discuss the numerical results and analyse the free energy of the different lattice solutions, showing that the triangular lattice has the lowest free energy of all the Abrikosov solutions studied. It is important to note that we are not able to show conclusively that we have found *the* ground state but we are able to find a state with lower free energy than the translationally invariant state and that has lowest energy within a large class of lattice solutions. In section 5 we conclude and give an outline of important future work.

2 Holographic setup

2.1 The finite temperature and hard wall backgrounds

The system we study is an Einstein-Yang-Mills theory on the (Poincaré patch of) an asymptotically AdS_5 geometry with an $SU(2)$ gauge field. The action is

$$S = \int d^5x \sqrt{-g} \left\{ \frac{1}{16\pi G_N} \left(R + \frac{12}{L^2} \right) - \frac{1}{4\hat{g}^2} \text{tr}(F_{\mu\nu}F^{\mu\nu}) \right\}, \quad (2.1)$$

where \hat{g} is the Yang-Mills coupling, G_N is the 5D gravitational constant and L is the AdS_5 radius. R and F are the Ricci scalar and Yang-Mills field strength respectively.

We consider the probe approximation, where the Yang-Mills term is small compared to the Einstein-Hilbert term, so that the backreaction of the gauge fields on the geometry can be neglected. We thus choose a fixed 5-dimensional background metric, given by

$$ds^2 = \frac{L^2}{u^2} \left(-f(u)dt^2 + dx^2 + dy^2 + dz^2 + \frac{du^2}{f(u)} \right), \quad (2.2)$$

where the asymptotically AdS region is at $u \rightarrow 0$. We study two different models. The first is a finite temperature model where the background is AdS Schwarzschild, first proposed in [39]. In this case, $f(u) = 1 - \frac{u^4}{u_H^4}$, where u_H is the location of the planar black hole horizon. The Hawking temperature of the black hole is $T = 1/\pi u_H$. The second model is the hard wall cutoff model,

proposed in [40, 41], where $f(u) = 1$ and the geometry terminates at a radial distance u_C . This model corresponds to a zero temperature theory ($u_H = \infty$), but it still has a scale u_C which corresponds to a confinement scale in the gauge theory. The intrinsic scales in these theories allow us to form a dimensionless magnitude for the magnetic field. This will be the parameter that we tune in order to find the instability of the spatially invariant ground state. Without loss of generality we can choose units where $u_H = 1$ in the finite temperature theory and $u_C = 1$ in the confining theory. Factors of u_H and u_C can then be restored through dimensional analysis. In the following the exact form of the metric is not important until we come to solving the numerical equations in the radial direction of AdS.

2.2 The Yang-Mills action

The relevant part of the action simplifies to

$$S = -\frac{1}{4\hat{g}^2} \int d^5x \sqrt{-g} \operatorname{tr} (F_{\mu\nu} F^{\mu\nu}) , \quad (2.3)$$

with the equations of motion

$$\nabla^\mu F_{\mu\nu}^a + \epsilon^{abc} \mathcal{A}^{b\mu} F_{\mu\nu}^c = 0 . \quad (2.4)$$

The $SU(2)$ gauge field is $\mathcal{A} = \mathcal{A}_\mu^a \tau^a dx^\mu$, for $a = 1 \dots 3$. We use the convention where the Lie algebra basis is given by $\tau^a = \frac{\sigma^a}{2i}$, with σ^a the Pauli matrices, and the structure constants f^{abc} are defined by $[\tau^a, \tau^b] = \epsilon^{abc} \tau^c$ so that $f^{abc} = \epsilon^{abc}$. With these definitions, the components of the field-strength tensor $F = d\mathcal{A} + \mathcal{A} \wedge \mathcal{A}$ become

$$F_{\mu\nu}^a = \partial_\mu \mathcal{A}_\nu^a - \partial_\nu \mathcal{A}_\mu^a + \epsilon^{abc} \mathcal{A}_\mu^b \mathcal{A}_\nu^c . \quad (2.5)$$

It will be important to understand how gauge transformations affect the system. Under a gauge transformation $e^{i\Lambda(x^\mu)}$, \mathcal{A} transforms as

$$\mathcal{A}_\mu \rightarrow \mathcal{A}_\mu + \delta \mathcal{A}_\mu = e^{i\Lambda} \mathcal{A}_\mu e^{-i\Lambda} - i \partial_\mu e^{i\Lambda} e^{-i\Lambda} . \quad (2.6)$$

When $\Lambda(x^\mu)$ is an infinitesimal transformation, this becomes

$$\delta \mathcal{A}_\mu^a = \mathcal{D}_\mu \Lambda^a = \partial_\mu \Lambda^a + \epsilon^{abc} \mathcal{A}_\mu^b \Lambda^c . \quad (2.7)$$

The gauge transformations give us the freedom to fix the gauge $\mathcal{A}_u^a = 0$. We work in this gauge from now on.

In this paper we look at the effect of a strong (flavour-)magnetic field given by $F_{xy}^3 = B$, with all other components of $F_{\mu\nu}^a$ vanishing. As we will see, when B becomes large³, other components of F become non-zero dynamically. To get a consistent set of equations we therefore consider a gauge field \mathcal{A} of the form

$$\mathcal{A} = \sum_{a=1,2,3, \mu=x,y} \mathcal{A}_\mu^a(x, y, u) \tau^a dx^\mu . \quad (2.8)$$

It turns out that we can turn off the t and z dependence of the gauge field and still have consistent equations. This simplifies the equations. Turning off the t dependence guarantees a static solution. Turning off the z dependence, where the z direction is parallel to the magnetic field, yields a lattice in the x, y -plane.

The action 2.3 has an $SU(2)$ gauge freedom. Choosing the solution $F_{xy}^3 = B$, with all other components vanishing, breaks this symmetry. Only $U(1)$ transformations of the form $\Lambda = \Lambda^3 \tau^3$ leave

³Since we have chosen the units where $u_H = 1$ or $u_C = 1$, B is a dimensionless quantity. Restoring the units, the statement is that $B u_H^2 = B/(\pi T)^2$ or $B u_C^2 \sim B/\Lambda_{QCD}^2$ is large, or that B is large compared to the radial scale of the background.

it invariant. For B large enough, all the components in 2.8 become nonzero due to the dynamics. We thus claim to have a superconductor, because the $U(1)$ symmetry is broken dynamically. Note however that it is technically a superfluid because the $U(1)$ gauge symmetry in the bulk theory gets mapped to a global symmetry in the field theory. Taking the linear combinations $\mathcal{E}_\mu^\pm = \mathcal{A}_\mu^1 \pm i\mathcal{A}_\mu^2$ gives fields that transform in the fundamental of the remaining gauge symmetry. It can be checked from 2.7 that $\mathcal{E}_\mu^\pm \rightarrow \mp i\Lambda^3 \mathcal{E}_\mu^\pm$ whenever $\Lambda = \Lambda^3 \tau^3$. Later on we work only with the fields \mathcal{E}^+ , which we rename to \mathcal{E} .

2.3 Perturbative expansion of the gauge fields

Substituting the ansatz 2.8 into equation 2.4 yields nine coupled partial differential equations in the variables x , y and u . Of these nine equations of motion, six are dynamical equations for each field $\mathcal{A}_{x,y}^{1,2,3}$, and three equations are constraints. The constraint equations arise from the equations of motion for the components $\mathcal{A}_u^{1,2,3}$, which were chosen to be zero using gauge symmetry.

In solving the PDE's, we follow the strategy of [2, 42], which works as follows. When the magnetic field B is smaller than some critical value B_c , the field configuration $\mathcal{A}_y^3 = xB$, $\mathcal{A}_x^3 = 0$ and $\mathcal{A}_{x,y}^{1,2} = 0$ solves the equations of motion. This is the normal phase of the superconductor. As shown in [1], the system enters a new phase when the magnetic field is increased beyond some critical value B_c . In this phase, the superconducting phase, the ground state has a non-trivial profile for all fields in the ansatz equation 2.8. We look for this configuration at some value of B infinitesimally above B_c , where the condensate is still small. This lets us do a perturbative expansion in a small parameter $\varepsilon \sim \frac{B-B_c}{B_c}$. For notational convenience we leave this parameter ε explicit when studying the expansion. However, it will be absorbed into the definition of the perturbative corrections to the fields when we come to minimising the energy. We thus write an ansatz for the expansion in the form

$$\mathcal{A}_y^3 = xB_c + \varepsilon \mathcal{A}_y^3 + \varepsilon^2 a_y^3 + \dots, \quad (2.9)$$

$$\mathcal{A}_\mu^a = \varepsilon \mathcal{A}_\mu^a + \varepsilon^2 a_\mu^a + \dots \quad \text{for } (a, \mu) \neq (3, y), \quad (2.10)$$

and solve the equations order by order in ε , as detailed in section 3.

2.4 Gauge field boundary conditions

The holographic dictionary relates field theory operators to gravity theory fields through the relation

$$e^{-W_{\text{CFT}}[\mathcal{A}^{(0)}]} = \langle e^{\int_{\partial \text{AdS}} \mathcal{A}_\mu^{(0)} J^\mu} \rangle = e^{-S_{\text{on-shell}}}. \quad (2.11)$$

The minus sign on the right-hand side is because we are in Euclidean space for simplicity. Here $\mathcal{A}^{(0)}$ is the value of the gauge field \mathcal{A} at the AdS boundary. It acts as a source in the boundary field theory. In our setup, the only source we want in the field theory comes from the component $\mathcal{A}_y^3 = xB$, producing the magnetic field. For the other components in 2.8, there should be no explicit source because we want to model spontaneous symmetry breaking. The spontaneous symmetry breaking results in a vev⁴,

$$\langle J^\mu \rangle = \left. \frac{\delta W_{\text{CFT}}}{\delta \mathcal{A}_\mu^{(0)}} \right|_{\mathcal{A}_\mu^{(0)}=0} = \left. \frac{\delta S_{\text{on-shell}}}{\delta \mathcal{A}_\mu^{(0)}} \right|_{\mathcal{A}_\mu^{(0)}=0} = - \int d^4x \frac{\partial \mathcal{L}}{\partial (\partial_u \mathcal{A}_\mu)} \Big|_{u=0} \quad (2.12)$$

The second equality is a generalisation to the radial coordinate of one of the steps in deriving the Hamilton-Jacobi equation. It relates the variation of final value of a generalised coordinate with respect to the on-shell action and the conjugate momentum at the final time.

⁴We also need to take holographic renormalisation into account to yield a finite on-shell action.

It is interesting to note that the on-shell action can be written as

$$S_{\text{on-shell}} = -\frac{1}{2\hat{g}^2} \int_{\partial \text{AdS}} d^d x \sqrt{-\gamma} n_\mu A_\nu^a F^{a\mu\nu} + \frac{1}{4\hat{g}^2} \int_{\text{AdS}} d^{d+1} x \sqrt{-g} \epsilon^{abc} A_\mu^a A_\nu^b F^{c\mu\nu} , \quad (2.13)$$

where we integrated by parts and substituted in the equations of motion. The second term on the right-hand side, the bulk term, is not present in non-interacting theories. In our case, however, it is present and nonzero even after using ansatz 2.8. This bulk term should seemingly influence the calculation of the condensate when varying with respect to the boundary value. It turns out that, due to the formula at the right of equality 2.12, it makes no contribution.

Equations 2.11 and 2.12 imply that in an expansion of the gauge fields near the AdS boundary, the leading term is the source and the subleading term is proportional to the vev. The field $\mathcal{A}_{x,y}^3$ has a boundary expansion given by

$$\mathcal{A}_{x,y}^3|_{u \rightarrow 0} = s_{x,y}^{(3)} + v_{x,y}^{(3)} u^2 + \dots , \quad (2.14)$$

where $s_{x,y}^{(3)}$ is the value of the source, which in this case is the externally applied magnetic field potential. $v_{x,y}^{(3)}$ is proportional to the vev corresponding to the magnetisation. We set the boundary conditions so that the applied magnetic field is not corrected by the higher order perturbations in ε , whereas the magnetisation will obtain a non-zero value.

Similarly, the fields $A_{x,y}^{1,2}$ have a boundary expansion given by

$$\mathcal{A}_{x,y}^{1,2}|_{u \rightarrow 0} = s_{x,y}^{(1,2)} + v_{x,y}^{(1,2)} u^2 + \dots , \quad (2.15)$$

where $s_{x,y}^{(1,2)}$ corresponds to the source of the operator that will condense to break the $U(1)$ symmetry. We adjust the boundary conditions in such a way that this vanishes. This means that the symmetry breaking is spontaneous. $v_{x,y}^{(1,2)}$ is proportional to the vacuum expectation value of this operator, which we read off to find the resulting supercurrent in the superconducting phase.

Boundary conditions are also imposed on the fields in the IR. In the case of the black hole background, we impose regularity at the horizon and in the case of the hard wall model we impose Neumann boundary conditions.

2.5 The gauge theory ground state energy

In finding the ground state, it is important to be able to calculate the energy of the field theory solution from the action. We would like to compare the solutions in the normal phase to those in the superconducting phase. The energy \mathcal{F} of the gauge theory solution is found by using the holographic dictionary. In the case of the finite temperature solution, we are in the canonical ensemble and we calculate the free energy, which is $\mathcal{F}/T = -\ln \mathcal{Z} = -S_{cl}$ with our conventions. Here $S_{cl} = -\frac{1}{4\hat{g}^2} \int d^5 x \sqrt{-g} F_{\mu\nu}^a F^{a\mu\nu}$ is the classical action. In the hard wall case, we are simply calculating the energy of the field configuration, which is defined in terms of the classical action in the same way. Since we are only interested in whether the energy of a particular superconducting solution is lower than that of the normal phase solution, we can simply calculate the difference $\Delta\mathcal{F} = \mathcal{F}_s - \mathcal{F}_n$ and thus do not need to implement holographic renormalisation. Here \mathcal{F}_s is the energy of the superconducting phase, while \mathcal{F}_n is the normal phase energy with $\mathcal{A}_y^3 = xB$ and all other components zero. We also need to take care of the fact that S_{cl} diverges when we perform the integral over the Minkowski directions. This is easy to fix by considering the energy density⁵ Ω , which is obtained by integrating S_{cl} only over the world volume of one lattice cell and dividing by its volume. Having explained how to calculate the energy of a field configuration, in the next section we turn to the problem of solving the equations of motion to find the ground state.

⁵We divide the free energy by T in the finite temperature model to get a dimensionless Ω . This means that in both models, our total dimensionless energy is simply $-S_{cl}$.

3 Solving the equations

3.1 The comparison with Ginzburg-Landau theory

Before turning to the equations of motion, it helps to first look at the Ginzburg-Landau equations for an analogy. In some suitable units defined in [2, 42], they are

$$\left(-i\nabla - \vec{A}\right)^2 \psi - \psi + |\psi|^2 \psi = 0 , \quad (3.1)$$

$$\nabla \times \nabla \times \vec{A} = -i(\bar{\psi}\nabla\psi - \psi\nabla\bar{\psi}) - |\psi|^2 \vec{A} . \quad (3.2)$$

Only the structure of these equations is important, so we have ignored constant factors. Here ψ is the wave function of Cooper pairs, and \vec{A} is the electromagnetic vector potential. The nine equations of motion in our system can be split into two groups that roughly correspond to the two equations above.

The first of the two groups, hereafter called the condensate equations, contains the six equations for the fields $\mathcal{A}_{x,y,u}^{1,2}$. The superconducting condensate of the dual field theory, which is like ψ above, is found by differentiating the on-shell action with respect to the boundary values of $\mathcal{A}_{x,y}^{1,2}$, as in equation 2.12. Of the six equations in this group, the dynamical equations are for $\mathcal{A}_{x,y}^{1,2}$ and the constraint⁶ equations are for $\mathcal{A}_u^{1,2}$. So this first group is analogous to equation 3.1. The analogy can be made more clear. As mentioned above, we can make the field definitions $\mathcal{E}_{x,y} = \mathcal{A}_{x,y}^1 + i\mathcal{A}_{x,y}^2$. Doing so allows us to combine the six real equations into three complex equations, two dynamical and one constraint. The constraint equation relates \mathcal{E}_x and \mathcal{E}_y such that there is only one complex degree of freedom left, which is analogous to the state ψ . All this is hard to see at the non-perturbative level, but it illustrates the strategy we follow for solving the equations at each order: we use the constraint equation to reduce the two dynamical equations into one, and then solve it.

The second group of equations, which we call the magnetic field equations, is for the fields $\mathcal{A}_{x,y,u}^3$, corresponding to \vec{A} in equation 3.2 above. There are three such equations, one of which is a constraint. At each order we will be able to use the constraint to separate the equations into one for \mathcal{A}_x^3 and one for \mathcal{A}_y^3 .

3.2 The gauge field perturbative expansion in more detail

Having defined the ansatz for our gauge potential in equation 2.9 we can learn more about the perturbative expansion by studying the non-linear structure of the equations of motion. The equation for \mathcal{A}_u^3 is

$$-\mathcal{A}_x^2 \partial_u \mathcal{A}_x^1 - \mathcal{A}_y^2 \partial_u \mathcal{A}_y^1 + \mathcal{A}_x^1 \partial_u \mathcal{A}_x^2 + \mathcal{A}_y^1 \partial_u \mathcal{A}_y^2 + \partial_y \partial_u \mathcal{A}_y^3 + \partial_x \partial_u \mathcal{A}_x^3 = 0 . \quad (3.3)$$

We see that the magnetic field components appear in the linear terms, while the condensate components appear in quadratic terms. This suggests that a contribution to the condensate components that is first order in the perturbative expansion influences a second order contribution in the magnetic field components. More generally, an odd order contribution to the condensate components influences an even order contribution to the magnetic field components.

This structure is common throughout all the equations of motion. It turns out that terms in the perturbative expansion of the magnetic field components that have an odd order vanish. The even order terms in the condensate components can then also be set to zero. We can thus constrain the expansion ansatz of equation 2.9 to

$$\begin{aligned} \mathcal{E}_{x,y} &= \varepsilon E_{x,y} + \varepsilon^3 e_{x,y} + \mathcal{O}(\varepsilon^5) , \\ \mathcal{A}_y^3 &= x B_c + \varepsilon^2 a_y^3 + \mathcal{O}(\varepsilon^4) , \\ \mathcal{A}_x^3 &= \varepsilon^2 a_x^3 + \mathcal{O}(\varepsilon^4) . \end{aligned} \quad (3.4)$$

⁶Recall that we have set $\mathcal{A}_u^a = 0$. However, its equations of motion still impose constraints on the other fields.

Here the calligraphic letters denote the non-perturbative fields. $E_{x,y}$ and $e_{x,y}$ are first and third order contributions to the condensate components, respectively, while $a_{x,y}^3$ are second order corrections to $\mathcal{A}_{x,y}^3$.

Because of this convenient expansion of the fields, the condensate components and the magnetic components decouple at each order. That means that at each order, we only need to work with fields we have already solved at previous orders. Our strategy is thus to solve for the fields in the following sequence:

$$\begin{array}{rclcl}
\mathcal{E}_{x,y} = & \boxed{\varepsilon E_{x,y}} & + & \boxed{\varepsilon^3 e_{x,y}} & + \mathcal{O}(\varepsilon^5) , \\
\mathcal{A}_y^3 = xB_c & + & & & + \mathcal{O}(\varepsilon^4) , \\
\mathcal{A}_x^3 = & & & \boxed{\begin{array}{c} \varepsilon^2 a_y^3 \\ \varepsilon^2 a_x^3 \end{array}} & + \mathcal{O}(\varepsilon^4) .
\end{array}$$

In the next section we start with the linear order solution, which will shed more light on the procedure that must be implemented at higher orders.

3.3 Solving the equations to linear order

Using the expansion 3.4 and keeping terms to linear order, we find that there are six remaining equations given (in complex form) by

$$0 = -iB_c x \partial_u E_y - \partial_y \partial_u E_y - \partial_x \partial_u E_x , \quad (3.5)$$

$$\begin{aligned}
0 = B_c^2 x^2 E_x - iB_c E_y + \left(\frac{f}{u} - f' \right) \partial_u E_x - f \partial_u^2 E_x - 2iB_c x \partial_y E_x \\
- \partial_y^2 E_x + iB_c x \partial_x E_y + \partial_x \partial_y E_y , \quad (3.6)
\end{aligned}$$

$$0 = 2iB_c E_x + \left(\frac{f}{u} - f' \right) \partial_u E_y - f \partial_u^2 E_y + iB_c x \partial_x E_x + \partial_x \partial_y E_x - \partial_x^2 E_y . \quad (3.7)$$

Here, as above, $f(u) = 1 - u^4$ for the AdS Schwarzschild model and $f(u) = 1$ for the hard wall model.

We can solve these equations by following Abrikosov [42]. The solution is given by

$$E_y = -iE_x , \quad (3.8)$$

$$E_x = \sum_{n=-\infty}^{\infty} C_n e^{-inky - \frac{1}{2} B_c \left(x - \frac{nk}{B_c} \right)^2} U(u) . \quad (3.9)$$

$U(u)$ is determined by solving

$$U'' + \left(\frac{f'(u)}{f(u)} - \frac{1}{u} \right) U' + \frac{B_c}{f(u)} U = 0 , \quad (3.10)$$

subject to the constraints $U(0) = 0$ and $U'(1) = 0$. For the AdS Schwarzschild model ($f(u) = 1 - u^4$), the latter constraint comes from imposing regularity at the horizon. It is possible to calculate B_c by numerically finding the value at which $U(u)$ satisfies these constraints. There is an infinite tower of solutions to B_c , but we are only interested in the lowest one, which is where the phase transition occurs. For further details on solving this equation in the AdS Schwarzschild model, see [1]. For the hard wall model, $f(u) = 1$ so the equation simplifies to the extent that it can be solved analytically, the solution being a Bessel function. Qualitatively the solutions for $U(u)$ in both models look very similar and we are only interested in their numerical form. For the AdS Schwarzschild model, we get $B_c \approx 5.1$, while we get $B_c \approx 5.8^7$ for the hard wall model.

⁷This is the zero of the Bessel function of the first kind $J_0(\sqrt{B})$.

It should be noted that the solution 3.9 for E_x agrees precisely (except for the factor of $U(u)$) with the linear order solution for the order parameter close to the upper critical magnetic field H_{c2} in the theory of type II superconductors, as seen in [42]. It is also the result found by Chernodub et al. in [7]. Depending on the values of the parameters C_n and k (to be determined by the higher order equations in the perturbative expansion), E_x corresponds to different inhomogeneous functions in the x, y -plane. We are particularly interested in finding those with lattice symmetries that represent evenly spaced vortices running in the z direction in the gauge theory.

3.4 The Abrikosov lattice solution

Before going beyond linear order, we discuss the possible solutions we can expect. The number of coefficients specifying a configuration can make the problem of finding the lowest energy solution unmanageable without making use of some symmetries. We can argue that, since nothing in the setup is explicitly breaking translational invariance in the x, y -directions, the solution should be a highly symmetric lattice. A nice review of how lattices can be formed from the Abrikosov solution (3.9) is given in [43]. There the authors explain that in order for $|E_x|$ to be a lattice solution, the coefficients C_n must have the same magnitude $|C_n|$ and moreover be periodic in some integer P , that is, $C_n = C_{n+P}$.

In [2], Abrikosov first studied the simplest solution, a square lattice. In this case, $P = 1$, implying that $C_n = C$ for all n , and $k = \sqrt{2\pi B_c}$. Later Kleiner et al. in [44] generalised the analysis by looking at $P = 2$, with $C_1 = \pm iC_0 = \pm iC$. This choice of coefficients specifies a general rhombic lattice, with the shape of the rhombus controlled by varying k . In particular, a square lattice can be obtained by choosing $k = \sqrt{\pi B_c}$. This square lattice is the same as Abrikosov's solution with $P = 1$, but it is rotated by $\pi/4$ and translated. A triangular lattice is obtained by choosing $k = 3^{1/4}\sqrt{\pi B_c}$.

To show how this works, we first substitute $P = 2$ and $C_1 = iC_0 = iC$ into the solution for E_x , which simplifies to

$$E_x = C \sum_{n=-\infty}^{\infty} e^{i\frac{\pi}{2}n^2 - ink y - \frac{1}{2}B_c(x - \frac{nk}{B_c})^2} U(u) . \quad (3.11)$$

It is then easy to see the symmetries $|E_x(x + [m + \frac{1}{2}q]L_x, y + [n + \frac{1}{2}q]L_y)| = |E_x(x, y)|$ for integers m, n and q . L_x and L_y are the lengths of the lattice cell in the x and y directions, and are given by $L_x = 2k/B_c$ and $L_y = 2\pi/k$. See figure 1.

We follow the approach of Kleiner et al, which is to compute the energy density of the lattice for a range of values of the ratio $L_x/L_y = k^2/\pi B_c$. This essentially means that we vary k . The energy is computed numerically from the analytic expressions we obtain at each order in the following sections. What we find agrees with their result that the triangular lattice has the lowest energy of the $P \leq 2$ solutions. When doing this, magnetic flux conservation is an important constraint. The total applied magnetic field per unit area is constant, and each lattice cell corresponds to a vortex with a single quantum of magnetic flux. This means that when comparing the energy of different lattices, we should make sure that they have the same magnetic flux per unit area, which in turn means that their lattice cells have the same area. Fortunately with this ansatz that is always the case since the area $L_x L_y = 4\pi/B_c$ is independent of k .

In the following sections we calculate analytic expressions for the higher order corrections to the gauge field. We keep P and the coefficients C_n general, except for imposing the periodicity condition $C_n = C_{n+P}$.

3.5 Higher order contributions to the energy

In order to find the ground state solution we must calculate the energy of the superconducting solutions and compare them to the normal phase solution. We can study the form of the energy as

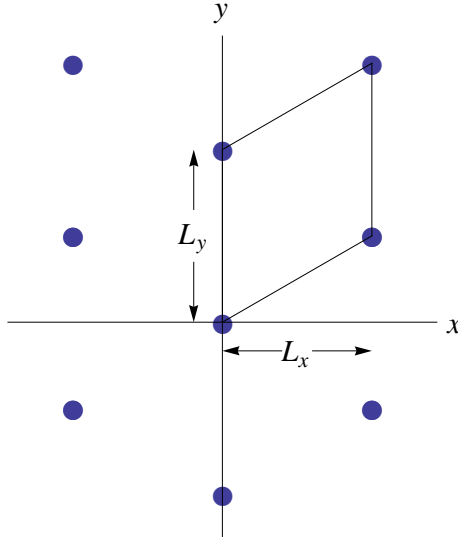


Figure 1. A lattice cell, illustrating the meanings of L_x and L_y for a fixed area cell.

defined in section 2.5 to see how far we must go in the perturbative expansion of the gauge fields. The energy has terms that are quadratic and quartic in the gauge potential. The quartic term ensures that the energy is bounded below, because it has a positive coefficient. The quartic terms have lowest perturbative contributions of order ε^4 . One might expect contributions of order ε^3 coming from the zeroth order magnetic field contribution multiplied by three first order corrections. However, from equation 3.4 it can be shown that such terms do not arise. Thus we should expect to expand to third order in $\mathcal{A}_{x,y}^{1,2}$ and fourth order in $\mathcal{A}_{x,y}^3$. However, it turns out that going to fourth order is not necessary because inserting ansatz 3.4 into the action of equation 2.3, we find that the only fourth order terms from $\mathcal{A}_{x,y}^3$ that appear at the fourth order of the action are proportional to $\sim \partial_y a_x^{(4)3} - \partial_x a_y^{(4)3}$. Here $a_x^{(4)3}$ and $a_y^{(4)3}$ are the fourth order corrections to \mathcal{A}_x^3 and \mathcal{A}_y^3 , respectively. This term respects the lattice symmetries, thus on performing the integration over the lattice cell to get the free energy density, it vanishes by Stokes' theorem.

We saw above that the parameters k and C_n in the solution 3.9 are not fixed by the equations of motion to linear order. This is due to the fact that to linear order, the different vortices do not interact. We can therefore not expect to fix any of the coefficients C_n or the spacing parameter k at this order. In fact, trying to calculate $\Delta\Omega$ to this order, which has no quartic terms in \mathcal{A} , one finds that the free energy density is not bounded below; increasing the overall magnitude of the condensate always decreases $\Delta\Omega$. To see which configuration, that is, which set of values for C_n and k , is energetically favourable, we clearly have to go beyond linear order.

3.6 Solving the equations to higher orders

In this section we solve the equations of motion up to third order in the perturbation parameter.

The second order corrections to the gauge fields contribute to the potentials \mathcal{A}_x^3 and \mathcal{A}_y^3 , that is, a_x^3 and a_y^3 in 3.4. These fields source the external magnetic field and the magnetisation. We impose that these corrections must vanish at the AdS boundary, so that the dual field theory has a constant applied magnetic field. We find however that they do not vanish throughout the bulk. In particular they develop non-vanishing subleading terms in the boundary expansion, representing a magnetisation in the field theory.

In appendix A we explain how the equations for the Fourier modes of the fields a_x^3 and a_y^3 can

be decoupled. This yields the following equations

$$u\partial_u \left(\frac{f}{u} \partial_u \hat{a}_{x,y}^3(m, n, u) \right) - \left(k^2 n^2 + \frac{4B_c^2 m^2 \pi^2}{k^2 P^2} \right) \hat{a}_{x,y}^3(m, n, u) + T_{x,y} e^{-\frac{k^2 n^2}{4B_c} + \frac{inm\pi}{P} - \frac{B_c m^2 \pi^2}{k^2 P^2}} \left(\sum_{l=0}^{P-1} e^{\frac{2ilm\pi}{P}} \bar{C}_l C_{l+n} \right) U^2 = 0, \quad (3.12)$$

where

$$T_x = -i \frac{\sqrt{B_c \pi}}{P} n, \quad T_y = 2i \frac{\pi^{3/2} B_c^{3/2}}{k^2 P^2} m, \quad (3.13)$$

and

$$a_{x,y}^3(x, y, u) = \sum_m \sum_n e^{-i \frac{2\pi m B_c}{Pk} x - ink y} \hat{a}_{x,y}^3(m, n, u). \quad (3.14)$$

As before, P defines the periodicity in the C_n . The parameters m and n correspond to the Fourier space levels of these fields. In order to calculate the solution $a_{x,y}^3(x, y, u)$ we will in theory need to solve these equations for all values of m and n . However, it will turn out to be sufficient to only study the first few Fourier modes. The numerical procedure for solving these will be explained in section 3.7

At third order we are studying the perturbative corrections to the condensate. Here we calculate the corrections e_x and e_y . It is reasonable to assume that the answer is of the form

$$\varepsilon E_x + \varepsilon^3 e_x = \varepsilon \sum_{n=-\infty}^{\infty} \left(C_n U(u) + \varepsilon^2 c_{x,n}(u) \right) e^{-ink y - \frac{1}{2} B_c \left(x - \frac{nk}{B_c} \right)^2}, \quad (3.15)$$

$$\varepsilon E_y + \varepsilon^3 e_y = \varepsilon \sum_{n=-\infty}^{\infty} \left(-i C_n U(u) + \varepsilon^2 c_{y,n}(u) \right) e^{-ink y - \frac{1}{2} B_c \left(x - \frac{nk}{B_c} \right)^2}, \quad (3.16)$$

where we have made use of equation 3.8 to relate the first order terms $C_n U(u)$ in \mathcal{E}_x and \mathcal{E}_y . $c_{(x,y),n}(u)$ is the first perturbative correction to the condensate where the u dependence is a function of n in contrast to the first order term.

We can write e_x and e_y in Fourier space, then use the three condensate equations discussed in section 3 to calculate these corrections. The one constraint equation can be used to decouple the other two equations. We then have one equation for $c_{x,n}(u)$ and one for $c_{y,n}(u)$. Further details are provided in appendix B.

3.7 Numerical solutions

Having separated the equations into ordinary differential equations in u by the method outlined in the appendices, we can now solve them numerically. Both the second and third order equations take the same general form, given by

$$u\partial_u \left(\frac{f}{u} \partial_u \phi \right) + G(m, n) \phi + H(m, n, u) = 0. \quad (3.17)$$

This equation can be solved numerically by picking some parameters for C_n and k that give a particular lattice and then using a shooting method to integrate from $u = 1$ (the horizon/hard wall cutoff) to $u = 0$ (the AdS boundary). It is an inhomogeneous second order differential equation, so there are two integration constants. The first is fixed by imposing regularity at the horizon or Neumann boundary conditions at the hard wall cutoff. This fixes the value of $\partial_u \phi(1)$. The second constant is obtained by demanding that $\phi(0) = 0$, so that the fields vanish at the AdS boundary. This vanishing corresponds to both the magnetic field strength corrections and the source for the condensate being set to zero. We fulfil this boundary condition by adjusting $\phi(1)$. Unlike in the

case of the first order equations, the equations here are not homogeneous and thus the source sets a scale with which the value $\phi(1)$ can be compared. Changing $\phi(1)$ in this case thus acts as more than just a scaling for the solution and so is used as the tuning parameter to satisfy the UV constraint.

For all of the equations, we can implement this procedure for arbitrary integers m and n , corresponding to the different Fourier modes of the gauge fields. This will then give a Fourier coefficient $\hat{a}_{x,y}^3(m, n, u)$ that can be used to determine $a_{x,y}^3(x, y, u)$. Fortunately we do not have to do the calculation for many different values of m and n , because as the values get large, the source term gets suppressed exponentially. This can be seen in equation 3.12 for the second order terms and is true also for the third order equation. For a vanishing source, the equations for \hat{a}_x^3 or \hat{a}_y^3 have only the trivial solution. This means that $\hat{a}_{x,y}^3(m, n, u)$ is negligibly small for large m or n , and we can therefore truncate the Fourier series for $a_{x,y}^3$ beyond $m, n \approx 3$.

4 Results

4.1 Finding the minimum energy state

As explained above, we wish to find the values of the parameters k , P and $C_n = C_{n+P}$ that give the minimum energy state. These parameters define the shape of the lattice. Our analysis is only valid for B slightly above B_c , where B_c was determined in section 3.3. The first step is thus to pick a value for B in this vicinity. We then choose a set of lattice parameters that give us the lattice solution we wish to consider. As mentioned in [43], for lattice solutions all the C_n must have the same magnitude C . We can therefore fix C_n up to the normalisation C , along with a value of k , according to the discussion in section 3.4. We then substitute these values into the energy density that was defined in section 2.5. It takes the form $\Delta\Omega = a_1\varepsilon C + a_2\varepsilon^2 C^2 + \dots$. At this point we see that we can redefine C by absorbing a factor of ε , which we call C_ε . C_ε is the only parameter left unfixed up to this point in the analysis. Here the a_i are values that are calculated numerically from substituting the solutions to the equations of motion into the expression for the energy derived in appendix C. $\Delta\Omega$ forms a Mexican hat potential, which is easy to minimise numerically. An illustration of this procedure is shown in figure 2. The plot in figure 3 shows the energy-minimising value of C_ε as a function of magnetic field near the phase transition at B_c . It shows that $C_\varepsilon \sim (B - B_c)^{\frac{1}{2}}$, so the condensate⁸ has a critical exponent of 1/2. A fit to the numerical data for the triangular lattice gives that $C_\varepsilon = 0.58(B - B_c)^{\frac{1}{2}}$ in the AdS Schwarzschild model and $C_\varepsilon = 0.53(B - B_c)^{\frac{1}{2}}$ in the hard wall model.

Having minimised with respect to C_ε for a given value of B and a given lattice configuration, we can plot the difference in the energy between the normal and superconducting states. Figure 4 shows $\Delta\Omega$, the difference between the energy density in the superconducting and normal phases, as a function of external magnetic field for two different lattices. The first lattice is square, and the second is triangular. Both are described in section 3.4.

The curves in figure 4 are the result of calculations in the AdS Schwarzschild model, but we get the same results up to a rescaling of the axes for the hard wall model. In the AdS Schwarzschild model, the critical magnetic field $B_c \approx 5.1$, while in the hard wall model $B_c \approx 5.8$. Each curve shows that the free energy density is proportional to $(B - B_c)^2$. This shows that the phase transition is second order, as expected if one looks at the analogous case in Ginzburg-Landau theory. There one can show ([45]) that the free energy is proportional to $(T - T_c)^2$, where T_c is the phase transition critical temperature.

⁸Note that only the combination εC is physically relevant, not C or ε independently.

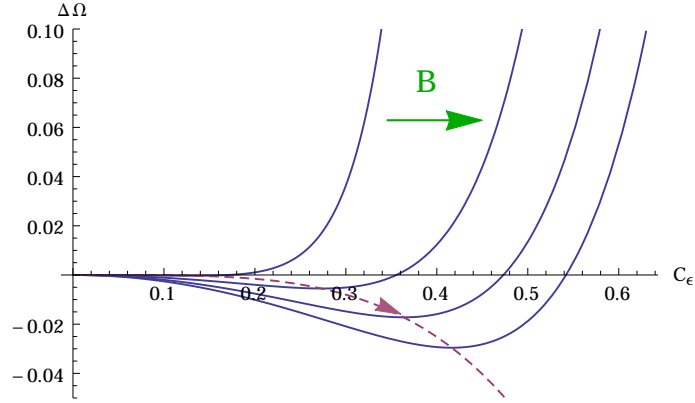


Figure 2. The change in energy density in units of temperature as a function of C_ε , the overall condensate scale. The leftmost curve corresponds to $B = B_c$, which is never negative for nonzero condensate. Curves for $B < B_c$ are similar. Increasing B beyond B_c yields the curves to the right, and we see the formation of a clear minimum of the energy that is lower than the energy of the normal phase. The dashed line traces out the minimum of each of these curves, which corresponds to the energetically preferred size of the condensate as a function of B . This plot was generated in the AdS Schwarzschild model for $P = 2$ and $k = 3^{\frac{1}{4}}\sqrt{\pi B}$, corresponding to a triangular lattice. B takes the values $B \approx B_c, 1.04B_c, 1.07B_c, 1.1B_c$ from left to right. Changing P and k to correspond to different lattices or using the hard wall model yields qualitatively similar results.

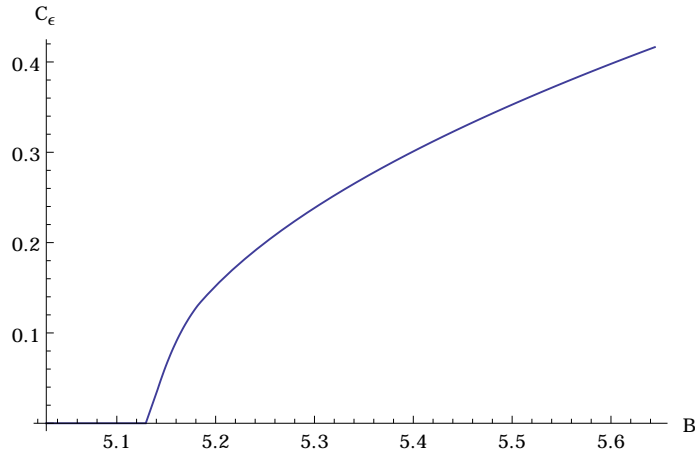


Figure 3. $C_\varepsilon \sim$ the overall condensate size for the AdS Schwarzschild solution in units of the temperature, as a function of the external magnetic field B . For $B < B_c$, the condensate is zero, and for B slightly above B_c , we see a $(B - B_c)^{\frac{1}{2}}$ scaling behaviour. This plot was generated for $P = 2$ and $k = 3^{\frac{1}{4}}\sqrt{\pi B}$, corresponding to a triangular lattice. The plot for different lattices in both the AdS Schwarzschild and hard wall models is the same, up to a scaling of the B and C_ε axes. For the triangular lattice, the AdS Schwarzschild model has scaling behaviour $C_\varepsilon = 0.58(B - 5.1)^{\frac{1}{2}}$ and the hard wall model has $C_\varepsilon = 0.53(B - 5.8)^{\frac{1}{2}}$.

4.2 An analysis of $P = 2$ solutions

We now specialise to the case where the periodicity of the C_n is $P = 2$. This describes a general rhombic lattice solution which includes both the triangular and square lattices. The $P = 1$ square lattice can be found within the $P = 2$ solutions up to translation and rotation. We here perform the analysis done in [44] as described at the end of section 3.4.

The energy difference as a function of R is plotted in figure 5. By looking at the form of

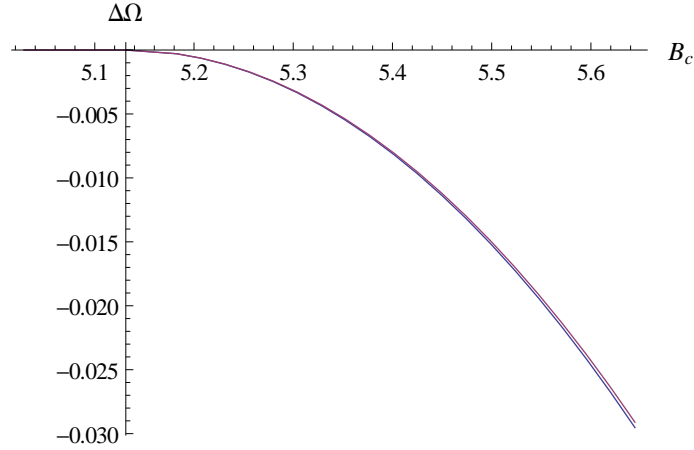


Figure 4. The change in energy density (compared to the normal phase) for the triangular and square lattices as the external applied magnetic field is varied. The phase transition happens at $B_c \approx 5.1$, which is where the coordinate axes are centred. $\Delta\Omega_{\text{square}} - \Delta\Omega_{\text{triangle}}$ is so small that the two plots are almost on top of each other. This is for the AdS Schwarzschild model, but the plots for the hard wall model are identical except for the scale on the axes. In the hard wall model, $B_c \approx 5.8$.

equation 3.11, it is possible to see that the triangular lattice occurs for $R = L_x/L_y = \sqrt{3}$ and $R = 1/\sqrt{3}$. In general, R and $1/R$ give the same lattice but with the x and y directions flipped. This is why figure 5 displays the symmetry $\Delta\Omega(R) = \Delta\Omega(1/R)$. The triangular lattice corresponds to a global minimum of the energy as a function of R , as seen from the figure. There is a local maximum for the square lattice, which is when $R = 1$. As $R \rightarrow \infty$ (or $R \rightarrow 0$), the free energy increases. Intuitively one can understand this by making use of the properties of Abrikosov vortices that we understand from type II superconductors. These vortices repel. Since $R \rightarrow \infty$ and $R \rightarrow 0$ correspond to elongating the rhombic lattice cell (while keeping the area constant) neighbouring vortices are squeezed together, and since they repel, this is energetically unfavourable.

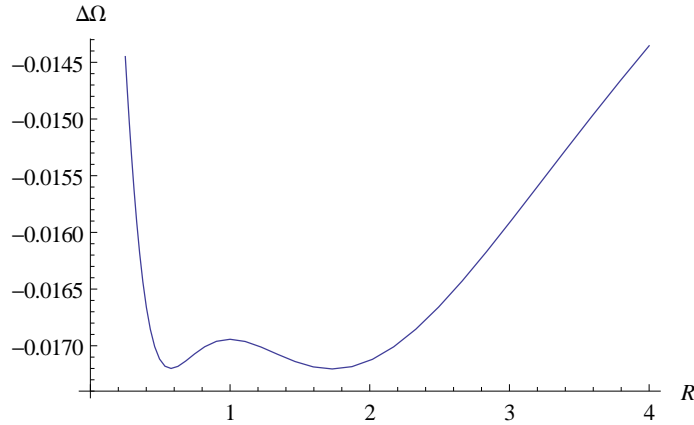


Figure 5. The change in free energy density as a function of $R = L_x/L_y$, the ratio of side lengths of a constant area lattice cell. This plot is for the AdS Schwarzschild model, but the plot for the hard wall model is identical up to a rescaling of the axes. When $R = 1$, the lattice is square and the free energy achieves a local maximum. When $R = \sqrt{3}$ and $1/\sqrt{3}$, the lattice is triangular and the free energy is at a global minimum. Note that the plot has the symmetry $\Delta\Omega(R) = \Delta\Omega(1/R)$, which simply corresponds to swapping the x, y -axes.

We can calculate the condensate in the minimum energy state using equation 2.12. The result, to linear order in ε , is

$$\langle J_x^+ \rangle = \frac{\delta S_{\text{on-shell}}}{\delta E_x^{(0)}} = \frac{L}{2\hat{g}^2} U_{\text{sub}} C_\varepsilon \sum_{n=-\infty}^{\infty} e^{-i\frac{\pi}{2}n^2 + ink y - \frac{1}{2}B_c(x - \frac{nk}{B_c})^2} \quad (4.1)$$

The AdS radius can be related to field theory quantities through the relation $L^4 = 2\lambda\alpha'^2$, where λ is the 't Hooft coupling and α' the string tension. The factor U_{sub} is equal to the subleading term in the boundary expansion of $U(u)$. Using equation 3.10 it is possible to show that

$$U_{\text{sub}} = B_c \int_0^{u_H} \frac{U(u)}{u} du, \quad (4.2)$$

so it can be determined numerically. In figure 6 we present the contour plot of $3^{\frac{1}{4}} \sqrt{8} \frac{\hat{g}^4}{L^2 U_{\text{sub}}^2 C_\varepsilon^2} |\langle J_x^+ \rangle|^2$, the modulus squared of the condensate in the x, y -plane for the minimum energy solution corresponding to the triangular lattice. The factors are chosen so that the maximum value is 1. Substituting in the numerical values, we find that the maximum value the condensate takes is $|\langle J_x^+ \rangle| = 1.0 \frac{L}{\hat{g}^2} (B - B_c)^{\frac{1}{2}}$ for the AdS Schwarzschild model, where $B_c \approx 5.1$, and $|\langle J_x^+ \rangle| = 1.3 \frac{L}{\hat{g}^2} (B - B_c)^{\frac{1}{2}}$ for the hard wall model, where $B_c \approx 5.8$.

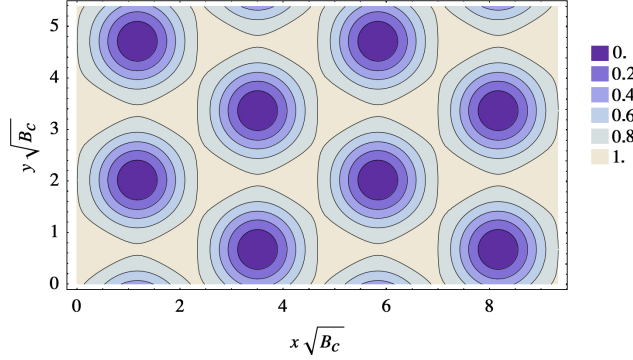


Figure 6. A contour plot of $3^{\frac{1}{4}} \sqrt{8} \frac{\hat{g}^4}{L^2 U_{\text{sub}}^2 C_\varepsilon^2} |\langle J_x^+ \rangle|^2$, the modulus squared of the field theory condensate dual to E_x in the ground state triangular lattice. At the center of the dark vortices, the condensate vanishes.

We could also plot the magnetisation of the ground state, which is found from the normalisable term in the boundary value expansion of $\partial_x a_y^3 - \partial_y a_x^3$. However, it takes the same form as the condensate and the numerics indicate that it differs only up to a scale.

5 Conclusion

In this work we have found a likely ground state for the black hole Yang-Mills instability analysed in [1]. The solution, being of a lattice form, clearly has much potential for analysis in condensed matter models, where the breaking of translational invariance has already been shown to be very important in getting realistic phenomenology. As we have explained, it also has possible implications for heavy ion collider physics. There are a number of interesting areas where we could apply similar techniques and perform further calculations to elucidate the phenomenology of the ground state found here.

It is certainly important to understand exactly how universal this result is. We have seen that the difference between the normal phase and superconducting phase energy density of this solution is, up to a scale, independent of the background geometry in the two models that we have studied

here. It would be very useful to understand precisely where this universality stems from and find how much we can deform the gravity solutions until the Abrikosov lattice is no longer the ground state.

In the present work we have analysed lattices with $P = 1$ and $P = 2$, corresponding to square and rhombic forms, respectively. Going to $P = 3$ requires a large increase in computational power. While this would be an interesting further calculation, the analogous cases of type II superconductivity and the model of Chernodub et al point to the triangular lattice being the true ground state. We thus expect higher P lattices to be energetically disfavoured.

Having found this solution, there are some extensions that can be made. It will now be possible to study time dependent fluctuations about the ground state. In order to do this we would have to introduce a second perturbative parameter in addition to the parameter ε used in the current work. This would be analogous to the parameter α' in a D-brane construction. This would allow us to study the transport properties of the lattice ground state, by looking at current-current correlation functions. If we wish to study the effect of the lattice on the shear viscosity to entropy density ratio, we would have to introduce gravitational back reaction in our model. Clearly this will be a much more involved calculation, with many non-linear couplings, but if we want to study the theory in a more realistic scenario, where the stress energy tensor also has a lattice structure, such a calculation would clearly be important.

It is expected that if the QCD vacuum is unstable to ρ meson condensation in extremely off-centre heavy ion collisions, then the timescale of the instability would not be enough to form a well-defined lattice. Abrikosov vortices may form, but the magnetic field would likely drop below the critical value before they had time to arrange themselves into a lattice. It would be very interesting to perform a real-time calculation in order to study the formation of the vortices and their movements as the magnetic field increased and decreased through the lifetime of a single off-centre collision.

Acknowledgements

Y.Y.B. was supported by MPG-CAS Doctoral Promotion Programme. The work of J.S. was supported by the European Union through a Marie Curie Fellowship. The work of J.E. and M.S. was supported in part by the DFG cluster of excellence ‘Origin and Structure of the Universe’ (www.universe-cluster.de). We thank Maxim Chernodub for useful discussions.

A Deriving the equations for $a_{x,y}^3$

We substitute the ansatz 3.4 into the full equations of motion and neglect terms beyond quadratic order in ε . To get rid of all appearances of E_y , we use the relation that $E_y = -iE_x$ from 3.8. Then we find that there are only three equations in which the fluctuations $a_{x,y}^3$ appear. We focus on those three equations.

The simplest equation of the three is the constraint equation, which came from the equation of motion for A_u^3 . To quadratic order, this equation is simply

$$\partial_u \partial_x a_x^3 + \partial_u \partial_y a_y^3 = 0 . \quad (\text{A.1})$$

The first thing to do is integrate by u . This gives an integration constant, but by the fact that both a_x^3 and a_y^3 must vanish at $u = 0$, this integration constant vanishes. So the even simpler constraint is

$$\partial_x a_x^3 + \partial_y a_y^3 = 0 . \quad (\text{A.2})$$

This is all we need to decouple the other two equations in a_x^3 and a_y^3 . These equations now become

$$0 = \frac{3}{2}E_x\partial_y\bar{E}_x + \frac{3}{2}\bar{E}_x\partial_yE_x - \frac{1}{2}iE_x\partial_x\bar{E}_x + \frac{1}{2}i\bar{E}_x\partial_xE_x + u\partial_u\left(\frac{f}{u}\partial_ua_x^3\right) + \partial_y^2a_x^3 + \partial_x^2a_x^3, \quad (\text{A.3})$$

$$0 = -B_c x \bar{E}_x E_x - \frac{1}{2}iE_x\partial_y\bar{E}_x + \frac{1}{2}i\bar{E}_x\partial_yE_x - \frac{3}{2}E_x\partial_x\bar{E}_x - \frac{3}{2}\bar{E}_x\partial_xE_x + u\partial_u\left(\frac{f}{u}\partial_ua_y^3\right) + \partial_y^2a_y^3 + \partial_x^2a_y^3, \quad (\text{A.4})$$

which are partial differential equations with sources that come from the linear order solutions. These two equations only differ by their source terms, so we will focus on a_x^3 . a_y^3 should be similar. Using the expression 3.9, we can see that the source term is periodic with $y \sim y + \frac{2\pi}{k}$. a_x^3 must have the same periodicity, so we can write it as a Fourier series,

$$a_x^3(x, y, u) = \sum_{n=-\infty}^{\infty} e^{-inky} \tilde{a}_x^3(x, n, u). \quad (\text{A.5})$$

The equation becomes

$$\sum_m -ie^{-\frac{1}{2}B_c(-\frac{km}{B_c}+x)^2 - \frac{1}{2}B_c(-\frac{k(n+m)}{B_c}+x)^2} kn\bar{C}_m C_{n+m} U^2 - k^2 n^2 \tilde{a}_x^3 + u\partial_u\left(\frac{f}{u}\partial_u\tilde{a}_x^3\right) + \partial_x^2\tilde{a}_x^3 = 0. \quad (\text{A.6})$$

We notice that the source term in this equation is periodic in the x -direction; $x \sim x + \frac{Pk}{B_c}$. This lets us expand \tilde{a}_x^3 as a Fourier series in x as well:

$$\tilde{a}_x^3 = \sum_m e^{-i\frac{2\pi m B_c}{Pk}x} \hat{a}_x^3(m, n, u). \quad (\text{A.7})$$

Writing the source term as a series lets us then obtain the equation 3.12 for the coefficients $\hat{a}_x^3(m, n, u)$.

Calling the source term $S(x)$, the naïve way of finding its Fourier coefficients is to use the formula

$$\tilde{S}_n = \frac{B_c}{Pk} \int_0^{\frac{Pk}{B_c}} e^{i\frac{2\pi n B_c}{Pk}x} S(x) dx. \quad (\text{A.8})$$

However, the source terms contains Gaussians, and those are much easier to integrate when the domain of integration is the entire real line. So we do the following trick. Doing a continuous Fourier transform on a periodic function gives a sum of δ -functions,

$$\begin{aligned} \int dx e^{ipx} S(x) &= \int dx e^{ipx} \sum_m e^{-i\frac{2\pi m B_c}{Pk}x} \tilde{S}_n \\ &= 2\pi \sum_m \tilde{S}_n \delta\left(p - \frac{2\pi m B_c}{Pk}\right). \end{aligned} \quad (\text{A.9})$$

The coefficients in front of the δ -functions are what we are looking for. We get

$$\int dx e^{ipx} S(x) = -\sqrt{\frac{\pi}{B_c}} \sum_{m,n} ie^{-\frac{k^2 n^2}{4B_c} + \frac{ikmp}{B_c} + \frac{iknp}{2B_c} - \frac{p^2}{4B_c}} kn\bar{C}_m C_{m+n} U^2. \quad (\text{A.10})$$

Using

$$\sum_{m=-\infty}^{\infty} f(m) = \sum_{m=-\infty}^{\infty} \sum_{l=0}^{P-1} f(Pm+l) \quad (\text{A.11})$$

and then using the symmetry $C_{i+P} = C_i$, the only m -dependence remaining in the sum comes from $e^{\frac{ikPmp}{B_c}}$. Making use of the identity

$$\sum_{m=-\infty}^{\infty} e^{imq} = 2\pi \sum_{m=-\infty}^{\infty} \delta(q - 2\pi m) \quad (\text{A.12})$$

and $\delta(\alpha x) = \frac{\delta(x)}{|\alpha|}$ gives us the sum over δ -functions from A.9. Then we can simply read off the coefficients \tilde{S}_n . This gives us the equation 3.12.

B Deriving the equations for $c_{x,n}$, $c_{y,n}$

The third order equations of motion are

$$0 = ia_x^3 \partial_u E_x + a_y^3 \partial_u E_x - iE_x \partial_u a_x^3 - E_x \partial_u a_y^3 + iB_c x \partial_u e_y + \partial_y \partial_u e_y + \partial_x \partial_u e_x, \quad (\text{B.1})$$

$$\begin{aligned} 0 = & -iB_c x a_x^3 E_x - 2B_c x a_y^3 E_x - \bar{E}_x E_x^2 - a_x^3 \partial_y E_x + 2ia_y^3 \partial_y E_x - a_y^3 \partial_x E_x \\ & - 2E_x \partial_y a_x^3 + iE_x \partial_y a_y^3 + E_x \partial_x a_y^3 + iB_c e_y - iB_c x \partial_x e_y - \partial_x \partial_y e_y \\ & - B_c^2 x^2 e_x + 2iB_c x \partial_y e_x + \partial_y^2 e_x + u \partial_u \left(\frac{f}{u} \partial_u e_x \right) \end{aligned} \quad (\text{B.2})$$

$$\begin{aligned} 0 = & B_c x a_x^3 E_x + i\bar{E}_x E_x^2 - ia_x^3 \partial_y E_x + 2a_x^3 \partial_x E_x - ia_y^3 \partial_x E_x \\ & + iE_x \partial_y a_x^3 + E_x \partial_x a_x^3 - 2iE_x \partial_x a_y^3 - 2iB_c e_x - iB_c x \partial_x e_x - \partial_x \partial_y e_x + \partial_x^2 e_y + u \partial_u \left(\frac{f}{u} \partial_u e_y \right). \end{aligned} \quad (\text{B.3})$$

The first of these is the constraint equation. We use it to relate e_x and e_y . In order to do this, we first simplify it by noticing that, since

$$e_y = \sum_{n=-\infty}^{\infty} c_{y,n}(u) e^{-inky - \frac{1}{2}B_c \left(x - \frac{nk}{B_c}\right)^2}, \quad (\text{B.4})$$

we have that $iB_c x \partial_u e_y + \partial_y \partial_u e_y = -i\partial_x \partial_u e_y$. We can then integrate the entire equation by u , imposing vanishing boundary conditions at the AdS boundary. The constraint equation then simplifies to

$$0 = -2i \frac{E_x}{U} J_x - 2 \frac{E_x}{U} J_y + ia_x^3 E_x + a_y^3 E_x + \partial_x e_x - i\partial_x e_y, \quad (\text{B.5})$$

where

$$J_{x,y}(x, y, u) = \int_0^u U(\tilde{u}) \partial_{\tilde{u}} a_{x,y}^3(x, y, \tilde{u}) d\tilde{u}. \quad (\text{B.6})$$

This allows us to eliminate e_x in equation B.3 (after differentiating it by x). We write each function as a Fourier series in y and find an equation for the coefficients $c_{y,n}$. At this point the equation still has an x dependence, which can be eliminated by multiplying the equation by $(nk - B_c x)$ to make it an even function in x and then integrating $\int_{-\infty}^{\infty} dx$. In doing so we use the solution for E_x and the form for e_y given by B.4, as well as the Fourier series representation of the other functions. Once this is done, we are left with an equation for e_y in the form 3.17.

The resulting equation for $c_{y,n}$ is

$$\begin{aligned}
0 = & \sum_{q,r=-\infty}^{\infty} \left\{ e^{-\frac{2\pi q (ik^2 P(n-r) + B_c \pi q)}{k^2 P^2}} \left[\frac{C_{n-r} \left(-2(k^2 Pr + 2iB_c \pi q) \hat{J}_{x,qr} \right)}{kP} \right. \right. \\
& + \frac{C_{n-r} \left((2ik^2 Pr - 4B_c \pi q) \hat{J}_{y,qr} + (2iB_c \pi q \hat{a}_x^3 + (-ik^2 Pr + 4B_c \pi q) \hat{a}_y^3) U \right)}{kP} \left. \right] \\
& - \frac{ie^{-\frac{k^2(3r^2 - 3rq + q^2)}{3B_c}} (3B_c + 2k^2 q(-2r + q)) \bar{C}_{n+q} C_{n+r} C_{n-r+q} U^3}{3\sqrt{3}B_c} \left. \right\} \\
& - B_c c_{y,n} + u \partial_u \left(\frac{f}{u} \partial_u c_{y,n} \right) , \tag{B.7}
\end{aligned}$$

where

$$\hat{J}_{i,qr}(u) = \int_0^u U(\tilde{u}) \partial_{\tilde{u}} \hat{a}_i^3(q, r, \tilde{u}) d\tilde{u} , \tag{B.8}$$

for $i = x, y$.

A similar procedure gives the constraint equation in terms of the coefficients,

$$\begin{aligned}
0 = & c_{x,n}(u) - i c_{y,n}(u) \\
& + \frac{1}{PkB_c} \sum_{q,r=-\infty}^{\infty} \left\{ e^{-\frac{2\pi q (ik^2 P(n-r) + B_c \pi q)}{k^2 P^2}} (-ik^2 Pr + 2B_c \pi q) C_{n-r} \right. \\
& \times \left(2\hat{J}_{x,qr} - 2i\hat{J}_{y,qr} - (\hat{a}_{x,qr}^3 - i\hat{a}_{y,qr}^3) U(u) \right) \left. \right\} . \tag{B.9}
\end{aligned}$$

Once the coefficients $c_{y,n}$ are found, we use this to calculate $c_{x,n}$.

C Calculating the energy

The difference between the energy of the superconducting phase and that of the normal phase is

$$\Delta \mathcal{F} = \frac{1}{4\hat{g}^2} \int d^5 x \sqrt{-g} \left(F_{\mu\nu}^a F^{a\mu\nu} \big|_{superconducting} - F_{\mu\nu}^a F^{a\mu\nu} \big|_{normal} \right) . \tag{C.1}$$

Note that for the AdS Schwarzschild model we implicitly divided by the temperature to make the energy dimensionless. We calculate the energy density by averaging over the domain $0 \leq y < \frac{2\pi}{k}$, $0 \leq x < \frac{Pk}{B_c}$, $0 \leq u \leq 1$ and $t, z \in \mathbb{R}$. Since the integrand is independent of t and z , the averaging amounts to simply dropping the integration over those variables. In the following expression we use

$$\mathcal{E}_{x,y} = \mathcal{A}_{x,y}^1 + i\mathcal{A}_{x,y}^2 = \sum_n \mathcal{C}_{(x,y),n}(u) e^{-ikny - \frac{1}{2}B_c(x - \frac{nk}{B_c})^2} , \tag{C.2}$$

we write $\mathcal{A}_x^3 = a_x^3$ and $\mathcal{A}_y^3 = xB + a_y^3$, and call the averaged energy $\Delta\Omega$. The result is

$$\begin{aligned}
4\hat{g}^2 \Delta\Omega = & \int du \left\{ \Omega_1(u) + \sum_{m,n=-\infty}^{\infty} [\Omega_2(m, n, u) + \Omega_3(m, n, u) + \Omega_4(m, n, u)] \right. \\
& \left. \sum_{m,n,p,q=-\infty}^{\infty} \Omega_5(m, n, q, r, u) \right\} , \tag{C.3}
\end{aligned}$$

where

$$\Omega_1 = \frac{\sqrt{\pi B}}{k P u} \sum_{l=0}^{P-1} \frac{B}{2} \left(\sum_{j=x,y} (f \partial_u \bar{\mathcal{C}}_{j,l} \partial_u \mathcal{C}_{j,l} + \bar{\mathcal{C}}_{j,l} \mathcal{C}_{j,l}) + 3(i \bar{\mathcal{C}}_{y,l} \mathcal{C}_{x,l} - i \bar{\mathcal{C}}_{x,l} \mathcal{C}_{y,l}) \right), \quad (\text{C.4})$$

$$\Omega_2 = \frac{1}{u} \left\| k n \hat{a}_x^3(m, n, u) - \frac{2 B m \pi}{k P} \hat{a}_y^3(m, n, u) \right\|^2 + \frac{f}{u} \sum_{j=x,y} \left\| \partial_u \hat{a}_j^3(m, n, u) \right\|^2, \quad (\text{C.5})$$

$$\begin{aligned} \Omega_3 = & \frac{\sqrt{\pi B}}{2 k^2 P^2 u} \sum_{l=0}^{P-1} e^{-\frac{k^2 m^2}{4 B} - \frac{i(2l+m)n\pi}{P} - \frac{B n^2 \pi^2}{k^2 P^2}} \left((3k^2 m P + 2i B n \pi) \hat{a}_x^3(n, m, u) \bar{\mathcal{C}}_{x,l+m} \mathcal{C}_{y,l} \right. \\ & + \hat{a}_x^3(n, -m, u) \bar{\mathcal{C}}_{y,l} ((3k^2 m P + 2i B n \pi) \mathcal{C}_{x,l+m} - 2i k^2 m P \mathcal{C}_{y,l+m}) \\ & + \hat{a}_y^3(n, -m, u) \mathcal{C}_{x,l+m} (-4i B n \pi \bar{\mathcal{C}}_{x,l} + (i k^2 m P + 6 B n \pi) \bar{\mathcal{C}}_{y,l}) \\ & \left. + \hat{a}_y^3(n, m, u) \bar{\mathcal{C}}_{x,l+m} \mathcal{C}_{y,l} (-i k^2 m P - 6 B n \pi) \right), \end{aligned} \quad (\text{C.6})$$

$$\begin{aligned} \Omega_4 = & -\frac{1}{4 k P u} \sqrt{\frac{\pi B}{2}} e^{-\frac{k^2(m^2+n^2)}{2 B}} \times \\ & \sum_{l=0}^{P-1} (\bar{\mathcal{C}}_{y,l+m} \bar{\mathcal{C}}_{y,l+n} \mathcal{C}_{x,l} \mathcal{C}_{x,l+m+n} - 2 \bar{\mathcal{C}}_{x,l+m} \bar{\mathcal{C}}_{y,l+n} \mathcal{C}_{x,l+m+n} \mathcal{C}_{y,l} + \bar{\mathcal{C}}_{x,l} \bar{\mathcal{C}}_{x,l+m+n} \mathcal{C}_{y,l+m} \mathcal{C}_{y,l+n}), \end{aligned} \quad (\text{C.7})$$

$$\begin{aligned} \Omega_5 = & \frac{\sqrt{\pi B}}{P k u} \sum_{l=0}^{P-1} e^{-\frac{k^2 m^2}{4 B} - \frac{i(2l+m)n\pi}{P} - \frac{B n^2 \pi^2}{k^2 P^2}} \times \\ & (\hat{a}_y^3(n-q, -(m+r), u) \hat{a}_y^3(q, r, u) \bar{\mathcal{C}}_{x,l} \mathcal{C}_{x,l+m} - \hat{a}_x^3(n-q, r, u) \hat{a}_y^3(q, m-r, u) \bar{\mathcal{C}}_{x,l+m} \mathcal{C}_{y,l} \\ & - \hat{a}_x^3(n-q, r, u) \hat{a}_y^3(q, -(m+r), u) \bar{\mathcal{C}}_{y,l} \mathcal{C}_{x,l+m} + \hat{a}_x^3(n-q, -(m+r), u) \hat{a}_x^3(q, r, u) \bar{\mathcal{C}}_{y,l} \mathcal{C}_{y,l+m}). \end{aligned} \quad (\text{C.8})$$

In these expressions, $\mathcal{C}_{x,n}$ and $\mathcal{C}_{y,n}$ are functions of u . Their complex conjugates are given by $\bar{\mathcal{C}}_{x,n}$ and $\bar{\mathcal{C}}_{y,n}$, respectively. All the infinite sums in the energy C.3 can be terminated at a small finite value because of exponential suppression in the $\Omega_{1\dots 5}$ terms.

In deriving this, it helps to make use of the formulae

$$\int_0^L dx \sum_{m=-\infty}^{\infty} e^{-\frac{B_c}{2}(x-mL)^2} = \int_{-\infty}^{\infty} dx e^{-\frac{B_c}{2}x^2}, \quad (\text{C.9})$$

$$\int_0^L dx \sum_{m,n=-\infty}^{\infty} e^{-\frac{B_c}{2}(x-\frac{mL}{P})^2 - \frac{B_c}{2}(x-\frac{nL}{P})^2} h(x, m, n) \quad (\text{C.10})$$

$$= \int_{-\infty}^{\infty} dx \sum_{l=0}^{P-1} \sum_{m=-\infty}^{\infty} e^{-\frac{B_c}{2}(x-\frac{mL}{P})^2 - \frac{B_c}{2}(x-\frac{lL}{P})^2} h(x, m, l), \quad (\text{C.11})$$

where the latter is valid whenever $h(x, m, n) = h(x+L, m+P, n+P)$.

References

- [1] M. Ammon, J. Erdmenger, P. Kerner, and M. Strydom, *Black Hole Instability Induced by a Magnetic Field*, *Phys.Lett.* **B706** (2011) 94–99, [[arXiv:1106.4551](#)].
- [2] A. Abrikosov, *On the Magnetic properties of superconductors of the second group*, *Sov.Phys.JETP* **5** (1957) 1174–1182.
- [3] G. T. Horowitz, J. E. Santos, and D. Tong, *Optical Conductivity with Holographic Lattices*, *JHEP* **1207** (2012) 168, [[arXiv:1204.0519](#)].

- [4] R. Flauger, E. Pajer, and S. Papanikolaou, *A Striped Holographic Superconductor*, *Phys.Rev.* **D83** (2011) 064009, [[arXiv:1010.1775](#)].
- [5] M. Chernodub, *Superconductivity of QCD vacuum in strong magnetic field*, *Phys.Rev.* **D82** (2010) 085011, [[arXiv:1008.1055](#)].
- [6] M. Chernodub, *Electromagnetically superconducting phase of QCD vacuum induced by strong magnetic field*, *AIP Conf.Proc.* **1343** (2011) 149–151, [[arXiv:1011.2658](#)].
- [7] M. Chernodub, J. Van Doorselaere, and H. Verschelde, *Electromagnetically superconducting phase of vacuum in strong magnetic field: structure of superconductor and superfluid vortex lattices in the ground state*, [arXiv:1111.4401](#).
- [8] N. Nielsen and P. Olesen, *An Unstable Yang-Mills Field Mode*, *Nucl.Phys.* **B144** (1978) 376.
- [9] J. Ambjorn and P. Olesen, *On Electroweak Magnetism*, *Nucl.Phys.* **B315** (1989) 606.
- [10] J. Ambjorn and P. Olesen, *A Condensate Solution Of The Electroweak Theory Which Interpolates Between The Broken And The Symmetric Phase*, *Nucl.Phys.* **B330** (1990) 193.
- [11] J. Ambjorn and P. Olesen, *Electroweak Magnetism: Theory And Application*, *Int.J.Mod.Phys.* **A5** (1990) 4525–4558.
- [12] S. K. Domokos and J. A. Harvey, *Baryon number-induced Chern-Simons couplings of vector and axial-vector mesons in holographic QCD*, *Phys.Rev.Lett.* **99** (2007) 141602, [[arXiv:0704.1604](#)].
- [13] S. Nakamura, H. Ooguri, and C.-S. Park, *Gravity Dual of Spatially Modulated Phase*, *Phys.Rev.* **D81** (2010) 044018, [[arXiv:0911.0679](#)].
- [14] W.-y. Chuang, S.-H. Dai, S. Kawamoto, F.-L. Lin, and C.-P. Yeh, *Dynamical Instability of Holographic QCD at Finite Density*, *Phys.Rev.* **D83** (2011) 106003, [[arXiv:1004.0162](#)].
- [15] O. Bergman, N. Jokela, G. Lifschytz, and M. Lippert, *Striped instability of a holographic Fermi-like liquid*, *JHEP* **1110** (2011) 034, [[arXiv:1106.3883](#)].
- [16] C. B. Bayona, K. Peeters, and M. Zamaklar, *A Non-homogeneous ground state of the low-temperature Sakai-Sugimoto model*, *JHEP* **1106** (2011) 092, [[arXiv:1104.2291](#)].
- [17] S. Takeuchi, *Modulated Instability in Five-Dimensional $U(1)$ Charged AdS Black Hole with R^{*2} -term*, *JHEP* **1201** (2012) 160, [[arXiv:1108.2064](#)].
- [18] H. Ooguri and C.-S. Park, *Holographic End-Point of Spatially Modulated Phase Transition*, *Phys.Rev.* **D82** (2010) 126001, [[arXiv:1007.3737](#)].
- [19] A. Donos and J. P. Gauntlett, *Helical superconducting black holes*, *Phys.Rev.Lett.* **108** (2012) 211601, [[arXiv:1203.0533](#)].
- [20] A. Donos and J. P. Gauntlett, *Black holes dual to helical current phases*, *Phys.Rev.* **D86** (2012) 064010, [[arXiv:1204.1734](#)].
- [21] M. Ammon, J. Erdmenger, S. Lin, S. Muller, A. O’Bannon, et al., *On Stability and Transport of Cold Holographic Matter*, *JHEP* **1109** (2011) 030, [[arXiv:1108.1798](#)].
- [22] A. Donos, J. P. Gauntlett, and C. Pantelidou, *Spatially modulated instabilities of magnetic black branes*, *JHEP* **1201** (2012) 061, [[arXiv:1109.0471](#)].
- [23] A. Donos and J. P. Gauntlett, *Holographic striped phases*, *JHEP* **1108** (2011) 140, [[arXiv:1106.2004](#)].
- [24] S. Bolognesi and D. Tong, *Monopoles and Holography*, *JHEP* **1101** (2011) 153, [[arXiv:1010.4178](#)].
- [25] P. Sutcliffe, *Monopoles in AdS*, *JHEP* **1108** (2011) 032, [[arXiv:1104.1888](#)].
- [26] D. Allahbakhshi, *On Holography of Julia-Zee Dyon*, *JHEP* **1109** (2011) 085, [[arXiv:1105.3677](#)].
- [27] K. Maeda, M. Natsuume, and T. Okamura, *Vortex lattice for a holographic superconductor*, *Phys.Rev.* **D81** (2010) 026002, [[arXiv:0910.4475](#)].

- [28] O. Domenech, M. Montull, A. Pomarol, A. Salvio, and P. J. Silva, *Emergent Gauge Fields in Holographic Superconductors*, *JHEP* **1008** (2010) 033, [[arXiv:1005.1776](#)].
- [29] J. M. Murray and Z. Tesanovic, *Isolated Vortex and Vortex Lattice in a Holographic p-wave Superconductor*, *Phys.Rev.* **D83** (2011) 126011, [[arXiv:1103.3232](#)].
- [30] S. S. Gubser and S. S. Pufu, *The Gravity dual of a p-wave superconductor*, *JHEP* **0811** (2008) 033, [[arXiv:0805.2960](#)].
- [31] M. Ammon, J. Erdmenger, M. Kaminski, and P. Kerner, *Superconductivity from gauge/gravity duality with flavor*, *Phys.Lett.* **B680** (2009) 516–520, [[arXiv:0810.2316](#)].
- [32] M. Ammon, J. Erdmenger, M. Kaminski, and P. Kerner, *Flavor Superconductivity from Gauge/Gravity Duality*, *JHEP* **0910** (2009) 067, [[arXiv:0903.1864](#)].
- [33] S. Chunlen, K. Peeters, P. Vanichchapongjaroen, and M. Zamaklar, *Instability of $N=2$ gauge theory in compact space with an isospin chemical potential*, *JHEP* **1301** (2013) 035, [[arXiv:1210.6188](#)].
- [34] D. Djukanovic, M. R. Schindler, J. Gegelia, and S. Scherer, *Quantum electrodynamics for vector mesons*, *Phys.Rev.Lett.* **95** (2005) 012001, [[hep-ph/0505180](#)].
- [35] M. Chernodub, *Spontaneous electromagnetic superconductivity of vacuum in strong magnetic field: evidence from the Nambu–Jona-Lasinio model*, *Phys.Rev.Lett.* **106** (2011) 142003, [[arXiv:1101.0117](#)].
- [36] V. Skokov, A. Y. Illarionov, and V. Toneev, *Estimate of the magnetic field strength in heavy-ion collisions*, *Int.J.Mod.Phys.* **A24** (2009) 5925–5932, [[arXiv:0907.1396](#)].
- [37] A. Bzdak and V. Skokov, *Event-by-event fluctuations of magnetic and electric fields in heavy ion collisions*, *Phys.Lett.* **B710** (2012) 171–174, [[arXiv:1111.1949](#)].
- [38] N. Callebaut, D. Dudal, and H. Verschelde, *Holographic rho mesons in an external magnetic field*, [[arXiv:1105.2217](#)].
- [39] E. Witten, *Anti-de Sitter space and holography*, *Adv.Theor.Math.Phys.* **2** (1998) 253–291, [[hep-th/9802150](#)].
- [40] J. Erlich, E. Katz, D. T. Son, and M. A. Stephanov, *QCD and a holographic model of hadrons*, *Phys.Rev.Lett.* **95** (2005) 261602, [[hep-ph/0501128](#)].
- [41] L. Da Rold and A. Pomarol, *Chiral symmetry breaking from five dimensional spaces*, *Nucl.Phys.* **B721** (2005) 79–97, [[hep-ph/0501218](#)].
- [42] A. Abrikosov, *Fundamentals of the Theory of Metals*. North-Holland, Amsterdam, 1988.
- [43] B. Rosenstein and D. Li, *Ginzburg-landau theory of type ii superconductors in magnetic field*, *Rev. Mod. Phys.* **82** (Jan, 2010) 109–168.
- [44] W. H. Kleiner, L. M. Roth, and S. H. Autler, *Bulk solution of ginzburg-landau equations for type ii superconductors: Upper critical field region*, *Phys. Rev.* **133** (Mar, 1964) A1226–A1227.
- [45] M. Tinkham, *Introduction to Superconductivity*. Robert E. Krieger Publishing Company, Malabar, Florida, 1980.